World Academy of Science, Engineering and Technology
International Journal of Electronics and Communication Engineering
Vol:4, No:3, 2010

Noise Performance of Millimeter-wave Silicon Based Mixed Tunneling Avalanche Transit Time (MITATT) Diode

Aritra Acharyya, Moumita Mukherjee and J. P. Banerjee

Abstract**—**A generalized method for small-signal simulation of avalanche noise in Mixed Tunneling Avalanche Transit Time (MITATT) device is presented in this paper where the effect of series resistance is taken into account. The method is applied to a millimeter-wave Double Drift Region (DDR) MITATT device based on Silicon to obtain noise spectral density and noise measure as a function of frequency for different values of series resistance. It is found that noise measure of the device at the operating frequency (122 GHz) with input power density of 10^{10} *Watt/m*^{2} is about *35 dB* for hypothetical parasitic series resistance of zero ohm (estimated junction temperature = *500 K*). Results show that the noise measure increases as the value of parasitic resistance increases.

Keywords**—**Noise Analysis, Silicon MITATT, Admittance characteristics, Noise spectral density.

I. Introduction

THE rapid development of the process technology of IMPATT device and fine line lithography have made possible the fabrication of this device having narrow depletion layer width working at high frequency mm-waves. IMPATTs are already established as powerful and efficient sources in various communication systems operating in millimetre-wave and submillimetre-wave bands of frequency. The millimeter-wave and submillimetre-wave frequencies have many fold advantages such as increased resolution, higher penetrating power through cloud, dust, fog etc, requirement of low power supply voltage and reduced system size [1-3]. Several window frequencies are observed in the millimetre-wave frequency range (30-300 GHz) such as 35, 94, 140, 220 GHz. A lot of research interest has therefore aroused to design and develop IMPATT diodes in MITATT modes at window frequencies, capable of delivering appreciable amount of millimeter wave power of the order of watts. Further sharp decrease of DC to RF conversion efficiency of the device at higher mm-wave frequencies of operation can be compensated by using impurity bumps in the depletion layer of flat profile structures leading to quasi Read hi-lo and lo-hi-lo devices [4]. The incorporation of impurity bump in the depletion layer of IMPATTs leads to constriction of avalanche zone and simultaneous increase of the breakdown field to very high values in the range of 6×10^7 *V/m* to 10×10^7 *V/m* [5]. Higher RF power output can be obtained from IMPATTs based on wider bandgap materials such as SiC, GaN and InP [6-8] as compared to those based on Silicon. Some theoretical studies on the RF performance of heterojunction IMPATTs based on III-V and IV-IV semiconductors as reported in the literature [9-11] show that heterojunction devices are suitable for generation of high millimeter wave power along with high conversion efficiency.

The IMPATT devices are inherently noisy due to the statistical nature of carrier generation by impact ionization. Tager [12] reported an approximate expression for the small signal noise spectrum in 1965. Later in the year 1966, Hines [13] proposed a small signal theory for noise analysis of IMPATT device assuming equal carrier ionization rates for electrons and holes. One pioneering work on small-signal noise analysis of IMPATT diode was reported by Gummel and Blue [14], for arbitrary doping profile and realistic values of the ionization rates as a function of electric field. Many other researchers like Haus et al [15], Kuvas [16] carried out significant works on the noise analysis of IMPATT diode. Dash and Pati [17] developed a method of noise analysis in Mixed Tunneling and Avalanche Transit Time (MITATT) device on the framework of well-known double iterative field maximum simulation technique first reported by Roy et.al [18-19]. They estimated noise spectral density of symmetrically doped DDR structures and also high-low quasi Read structures of Si MITATTs at the assumed junction temperature of 200^0C. The effect of parasitic series resistance of the device was not considered in their method [17]. In the present paper the authors have adopted a similar approach to carry out the noise analysis of an asymmetrically doped flat-profile Si MITATT device on the framework of Gummel-Blue technique [14] where the effect of series resistance is taken into account.

Rest of the paper is organised as follows. In the next section the DC and small-signal simulation method of the MITATT device is described. Results and discussions are provided in later section. Finally a conclusion is provided at the end of the paper.

II. DC and Small-signal Simulation Method

The authors have adopted a double iterative field-maximum method [5, 18-19] to study the MITATT mode operation of the device. MBE growth technique for development of *p-n*

Aritra Acharyya is with Institute of Radio Physics and Electronics, University of Calcutta, 92, APC Road, Kolkata 700009, India. (Phone: 91-9432979721, E-mail: ari_besu@yahoo.co.in).

Moumita Mukherjee is with CMSDS, Institute of Radio Physics and Electronics, University of Calcutta, 1, Girish Vidyaratna Lane, Kolkata 700009, India (E-mail: m_mukherjee07@rediffmail.com).

Professor (Dr.) J. P. Banerjee is with Institute of Radio Physics and Electronics, University of Calcutta, 92, APC Road, Kolkata 700009, India (E-mail: jpbanerjee06@rediffmail.com).

junction in included in the present modeling. At mm-wave region, since the device is operated at a higher bias current density, the junction temperature of the device increases above the room temperature. Thus the authors estimated the rise in junction temperature considering the effect of p^+ and n^+ contact metals. For this purpose a one dimensional heat-flow analysis of IMPATT device is carried out [20]. It is found that the device junction temperature at *94 GHz* rises to *500 K*. Thus the authors have designed the device at *500 K* to study the avalanche noise in W-band IMPATT device. Another consequence of high current operation is that the mobile space charge may degrade the performance seriously. The authors have optimized the bias current by several computer runs to minimize the effect of mobile space charge.

One-dimensional model of a reverse biased p^+pnn^+ DDR IMPATT device is shown in Fig. 1. In Fig. 1, x_L/x_R is the position where the electron energy in the valence/conduction band equals the energy corresponding to the bottom/top of the conduction/valance band at the n-side/p-side edge of the depletion layer. W is the total depletion width of the device and x_j is the position of the *p-n* junction. Poisson's equation including mobile space charge [21-22] in the depletion layer of the diode is given as,

$$\frac{d\xi}{dx} = \frac{q}{\varepsilon}\left(N_D - N_A + p(x) - n(x)\right) \tag{1}$$

Where, N_D = Ionized donor density, N_A = Ionized acceptor density, so $q.N_{dop} = q.(N_D - N_A)$ = net impurity space charge, $p(x)$ and $n(x)$ are hole and electron densities respectively. ξ_p is the portion of the electric field caused by the space charge of the mobile carriers, thus ξ_p is the total electric field minus the field associated with the impurity space charge [14],

$$\xi_p = \xi - \frac{q}{\varepsilon}\int N_{dop}\ \ dx \tag{2}$$

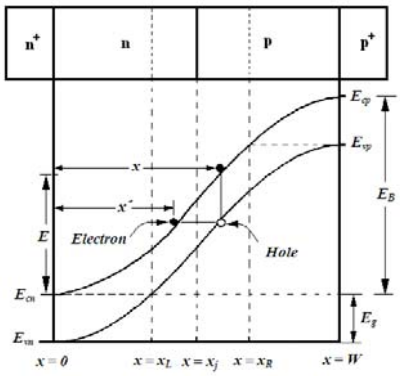

Fig. 1 One-dimensional model of a reverse biased IMPATT Diode [Showing the Tunnelling Positions of Electrons and Holes].

The total current density is the sum of conduction and displacement currents,

$$J = J_n + J_p + \frac{\partial}{\partial t}(\varepsilon\xi) = q\left(v_p p + v_n n\right) + \frac{\partial}{\partial t}(\varepsilon\xi) \tag{3}$$

Where, $J_p = qv_p p$ = hole current density and $J_n = qv_n n$ = electron current density. Equations (1) and (3) is solved for hole and electron concentrations in terms of the electric field ξ_p and given by [14],

$$p = \frac{J - \left(\frac{\partial}{\partial t} - \varepsilon v_n \frac{\partial}{\partial x}\right)\xi_p}{q\left(v_p + v_n\right)} \tag{4}$$

$$n = \frac{J - \left(\frac{\partial}{\partial t} + \varepsilon v_p \frac{\partial}{\partial x}\right)\xi_p}{q\left(v_p + v_n\right)} \tag{5}$$

Carrier Continuity equations in MITATT mode of operation can be written as,

$$\frac{\partial p}{\partial t} = -\left(\frac{1}{q}\right)\left(\frac{\partial J_p(x)}{\partial x}\right) + G_{Ap}(x) + G_{Tp}(x) + \gamma_p(x) + U_p \tag{6}$$

$$\frac{\partial n}{\partial t} = \left(\frac{1}{q}\right)\left(\frac{\partial J_n(x)}{\partial x}\right) + G_{An}(x) + G_{Tn}(x) + \gamma_n(x) - U_n \tag{7}$$

The avalanche process can be considered as combination of a noiseless generation rate G_A (given by (8)) and a noisy generation rate $\gamma = \gamma_p = \gamma_n$,

$$G_A(x) = G_{An}(x) = G_{Ap}(x) = \alpha_n(x)v_n(x)n(x) + \alpha_p(x)v_p(x)p(x) \tag{8}$$

α_n and α_p are electron and hole ionization rates. v_n and v_p are respective saturated drift velocities. U_n and U_p are the recombination rates of the electrons and holes respectively. Recombination effects are not included in the analysis since the transit time of carriers in the depletion layer of an IMPATT diode is several orders of magnitude shorter than the recombination time. So, the carrier continuity equation in the presence of noise in MITATT mode can be written as,

$$\frac{\partial(p+n)}{\partial t} + \frac{1}{q}\frac{\partial}{\partial x}\left(J_p - J_n\right) = 2\left(G_A(x) + \gamma(x)\right) + G_{Tn}(x) + G_{Tp}(x) \tag{9}$$

In this analysis the tunneling generation rate for electrons [$G_{Tn}(x)$] is obtained from quantum mechanical considerations as reported in [23-24]. Thus,

$$G_{Tn}(x) = a_T \xi^2(x) exp\left(-\frac{b_T}{\xi(x)}\right) \tag{10}$$

Where the coefficients a_T and b_T are given by,

$$a_T = \frac{q^2}{8\pi^3\hbar^2}\left(\frac{2m^*}{E_g}\right)^{\frac{1}{2}} \tag{11}$$

$$b_T = \frac{1}{2q\hbar}\left(\frac{m^* E_g^{\ 3}}{2}\right)^{\frac{1}{2}} \tag{12}$$

The symbols used in equations (10), (11) and (12) carry their usual significance. The tunneling generation rate for holes can be obtained from Fig. 1. The phenomenon of tunneling is instantaneous and the tunnel generation rate for holes is related with that for electrons i.e. $G_{Tp}(x) = G_{Tn}(x')$. The tunnel generation of an electron at x' is simultaneously associated with the generation of a hole at x, where $(x - x')$ is the spatial separation between the edge of conduction band and valence band at the same energy. If E is the measure of

energy from the bottom of the conduction band on the n-side and the vertical difference between x and x' is E_g, x' can be easily obtained from Fig. 1 as [5],

$$x = x'\left(1-\frac{E_g}{E}\right)^{-\frac{1}{2}} \qquad \text{for } 0 \le x \le x_j \tag{13}$$

$$x = W-(W-x')\left(1+\frac{E_g}{E_B-E}\right)^{-\frac{1}{2}} \qquad \text{for } x_j \le x \le W \tag{14}$$

The hole generation rate due to tunneling is zero in the region defined by $0 \le x \le x_L$ (Fig. 1) as electrons in the valance band have no available states in the conduction band for tunneling. Similarly, non-availability of states in the conduction band for tunneling to take place in the region $x_R \le x \le W$ (Fig. 1) makes no contribution of tunnel generated electrons in this region [5]. The expressions for electron and hole current densities are given by,

$$J_p = qpv_p - qD_p\left(\frac{\partial p}{\partial x}\right) \tag{15}$$

$$J_n = qnv_n + qD_n\left(\frac{\partial n}{\partial x}\right) \tag{16}$$

Where D_n and D_p are the diffusion constants of electrons and holes respectively. In this analysis diffusion current components are neglected for simplicity, as in this case diffusion current components are very much smaller than drift current components. So using the relations $J_n = qnv_n$ and $J_p = qpv_p$ the steady-state carrier continuity equations are written as [Under DC conditions, $\frac{\partial n}{\partial t} = \frac{\partial p}{\partial t} = 0$],

$$\frac{dJ_p(x)}{dx} = \alpha_n(x)J_n(x) + \alpha_p(x)J_p(x) + qG_T(x') + q\gamma(x) \tag{17}$$

$$\frac{dJ_n(x)}{dx} = -\alpha_n(x)J_n(x) - \alpha_p(x)J_p(x) - qG_T(x) - q\gamma(x) \tag{18}$$

The following equations can be formed by using $J = J_n + J_p = Constant$ and $P(x) = [J_p(x) - J_n(x)] / J$ in equations (17) and (18),

$$\frac{\partial P(x)}{\partial x} = (\alpha_n+\alpha_p)-(\alpha_n-\alpha_p)P(x)+\frac{q}{2J}\left(G_T(x)+G_T(x')\right)+\frac{2q}{J}\gamma(x) \tag{19}$$

Now $(p - n)$, i.e. the mobile space-charge concentration at any space point can be obtained from (17) and (18) as,

$$q\frac{\partial(p-n)}{\partial x} = J\left(\frac{\alpha_n}{v_n}+\frac{\alpha_p}{v_p}\right)-q(\alpha_n-\alpha_p)(p-n) + q\left(\frac{G_T(x)}{v_n}+\frac{G_T(x')}{v_p}\right)+q\gamma(x)\left(\frac{1}{v_n}+\frac{1}{v_p}\right)+\frac{\partial \xi}{\partial x}K \tag{20}$$

Where, K is a correction factor whose value depends on the type of the semiconductor base material. In the case on Si, variation of drift velocity for electrons and holes with electric field has form [25],

$$v_{n,p} = v_{sn,sp}\left[1-exp\left(\frac{-\mu_{n,p}\xi}{v_{sn,sp}}\right)\right] \tag{21}$$

For which the correction factor is given by,

$$K = \frac{J_p\mu_p}{v_p}\left(\frac{1}{v_{sp}}-\frac{1}{v_p}\right)-\frac{J_n\mu_n}{v_n}\left(\frac{1}{v_{sn}}-\frac{1}{v_n}\right) \tag{22}$$

The DC analysis of DDR IMPATT is first carried out by using a double iterative field maximum computer method [5, 18]. In this method the computation starts from the location of field maximum near the metallurgical junction. The spatial distributions of both DC electric field and carrier current densities in the depletion layer are obtained by using the above method, which involves iteration over the magnitude of field maximum (ξ_m) and its location in the depletion layer. A software package has been developed for simultaneous numerical solution of Poisson's equation, combined current continuity equations and the space charge equation subject to appropriate boundary conditions by taking into account the effects of mobile space charge [21-22] and tunneling [5]. Thus the electric field and carrier current density profiles are obtained for DDR device operating in both IMPATT and MITATT modes. The boundary conditions for the electric field at the depletion layer edges are given by (Fig. 2),

$$\xi(0) = 0 \quad and \quad \xi(W) = 0 \tag{23}$$

Where, 0 and W define the p^+ and n^+ edges of the depletion layer. The boundary conditions for normalized current density $P(x) = (J_p - J_n)/J_0$ at the edges are given by,

$$P(0) = \left(\frac{2}{M_p}-1\right) \; and \; P(W) = \left(1-\frac{2}{M_n}\right) \tag{24}$$

Where, $M_p = J_0 / J_{ps}$ = hole current multiplication factor and $M_n = J_0 / J_{ns}$ = electron current multiplication factor. The necessary device equations are simultaneously solved satisfying the appropriate boundary conditions given in (23) and (24). The field dependence of electron and hole ionization rates (α_n and α_p) and saturated drift velocities of electron (v_{sn}) and holes (v_{sp}) at *500 K* are incorporated in the simulation of DC electric field and carrier currents density profiles. The conversion efficiency is calculated from the semi quantitative formula [26],

$$\eta(\%) = \frac{2m}{\pi}\times\frac{V_D}{V_B} \tag{25}$$

Where, V_D = Voltage drop across the drift region, V_B = Breakdown voltage and m is the RF voltage modulation index. Avalanche breakdown takes place when the electric field at the junction is large enough such that the charge multiplication factors (M_n, M_p) become infinitely large ($\approx 10^6$). The breakdown voltage is obtained by integrating the electric field profile over the total depletion layer width, i.e.,

$$V_B = \int_0^W \xi(x)dx \tag{26}$$

The high-frequency analysis of DDR IMPATT diode is carried out to obtain distribution of negative resistivity in the depletion layer which provides considerable insight into the high frequency performance and the possible measure to improve the same. The range of frequency for which the device exhibits negative conductance is obtained from the admittance plot. The DC parameters are fed as input data for

the small signal analysis. The depletion layer edges of the device are fixed from the DC analysis and taken as the starting and end points for the small signal analysis. Two second order differential equations are framed by resolving the diode impedance $Z(x,\omega)$ into its real part $R(x,\omega)$ and imaginary part $X(x,\omega)$ [5, 19] given by,

$$\frac{\partial^2 R}{\partial x^2}+\left[\alpha_n(x)-\alpha_p(x)\right]\frac{\partial R}{\partial x}-2r_n\left(\frac{\omega}{\bar{v}}\right)\frac{\partial X}{\partial x}+\left[\left(\frac{\omega^2}{\bar{v}^2}\right)-H(x)-\frac{qr_p}{\bar{v}\varepsilon}\left(G_T'(x)+G_T'(x')\right)\right]R-2\bar{\alpha}\left(\frac{\omega}{\bar{v}}\right)X-2\left(\frac{\bar{\alpha}}{\bar{v}\varepsilon}\right)=0 \quad (27)$$

$$\frac{\partial^2 X}{\partial x^2}+\left[\alpha_n(x)-\alpha_p(x)\right]\frac{\partial X}{\partial x}-2r_n\left(\frac{\omega}{\bar{v}}\right)\frac{\partial R}{\partial x}+\left[\left(\frac{\omega^2}{\bar{v}^2}\right)-H(x)-\frac{qr_p}{\bar{v}\varepsilon}\left(G_T'(x)+G_T'(x')\right)\right]X+2\bar{\alpha}\left(\frac{\omega}{\bar{v}}\right)R+2\left(\frac{\omega}{\bar{v}^2\varepsilon}\right)=0 \quad (28)$$

The boundary conditions for R and X are given by: [n side & p side respectively]

$$\frac{\partial R}{\partial x}+\frac{\omega X}{v_{ns}}=-\left(\frac{1}{v_{ns}\varepsilon}\right) \text{ and } \frac{\partial X}{\partial x}-\frac{\omega R}{v_{ns}}=0 \quad \text{at } x=0 \quad (29)$$

$$\frac{\partial R}{\partial x}-\frac{\omega X}{v_{ps}}=\left(\frac{1}{v_{ps}\varepsilon}\right) \text{ and } \frac{\partial X}{\partial x}+\frac{\omega R}{v_{ps}}=0 \quad \text{at } x=W \quad (30)$$

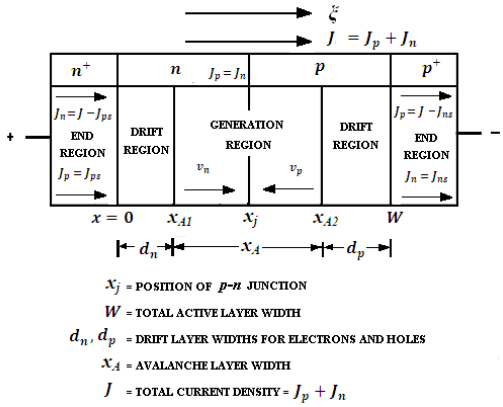

Fig. 2 Different active regions of DDR IMPATT device.

Where, $Z(x,\omega) = R(x,\omega) + i\,X(x,\omega)$. A double-iterative simulation scheme is used to solve those equations simultaneously by satisfying the boundary conditions. The device negative resistance (Z_R) and reactance (Z_x) are computed through the numerical integration of the $R(x)$ and $X(x)$ profiles over the space-charge layer width, W. Thus,

$$Z_R=\int_0^W R\,dx \quad and \quad Z_X=\int_0^W X\,dx \quad (31)$$

The negative conductance ($-G$), Susceptance (B) and the quality factor (Q_P) of the device are evaluated by using the following relations:

$$\left|-G(\omega)\right|=\frac{Z_R}{\left(Z_R^{\,2}+Z_X^{\,2}\right)} \quad (32)$$

$$\left|B(\omega)\right|=\frac{-Z_X}{\left(Z_R^{\,2}+Z_X^{\,2}\right)} \quad (33)$$

$$Q_p=-\left(B/G\right)_{at\ \ peak\ \ frequency} \quad (34)$$

It may be noted that both $-G$ and B are normalized to the area of the diode. At the resonant frequency of oscillation, the maximum RF power output (P_{RF}) from the device is calculated by using the following expression:

$$P_{RF}=\frac{1}{2}.V_{RF}^2.\left|G_p\right|.A \quad (35)$$

Where, V_{RF} is the amplitude of the RF swing ($V_{RF} = V_B/2$, assuming *50%* modulation of the breakdown voltage V_B), G_p is the diode negative conductance at the operating frequency and A is the junction area of the diode (junction diameter of the device is taken as *35 μm* [29] for W-band IMPATT device).

The present method is free from any simplifying assumptions and it takes into account the MBE grown realistic doping profiles, recently reported values of material parameters of silicon [27] at *500 K* and the effect of mobile space charge [21-22].

III. Noise Simulation Method

The random nature of the impact ionization process is the main source of noise in avalanche transit time device. This random impact ionization process gives rise to fluctuations in the DC current and DC electric field. These random fluctuations in the DC values of current and electric field appear as small-signal components to their DC values even when no voltage variation has been applied at the diode. Open circuit condition with no applied small-signal voltage is considered for the noise analysis in MITATT mode of the device. Expressing small-signal AC field, $e = e_r + ie_i$, two second order differential equation s are formed for real and imaginary parts of the noise field following standard procedure [17] the second order differential equations for real and imaginary parts of the noise electric field are obtained as,

$$D^2e_r(x,x')+\left[\alpha_n(x)-\alpha_p(x)\right]De_r(x,x')-\frac{2r_n\omega}{\bar{v}}De_i(x,x')+\left[\frac{\omega^2}{\bar{v}^2}-H(x)-\frac{qr_p}{\bar{v}\varepsilon}\left(G_T'(x)+G_T'(x')\right)\right]e_r(x,x')-\frac{2\bar{\alpha}(x)\omega}{\bar{v}}e_i(x,x')=\frac{2qr_p\gamma(x')}{\bar{v}\varepsilon} \quad (36)$$

$$D^2e_i(x,x')+\left[\alpha_n(x)-\alpha_p(x)\right]De_i(x,x')+\frac{2r_n\omega}{\bar{v}}De_r(x,x')+\left[\frac{\omega^2}{\bar{v}^2}-H(x)-\frac{qr_p}{\bar{v}\varepsilon}\left(G_T'(x)+G_T'(x')\right)\right]e_i(x,x')-\frac{2\bar{\alpha}(x)\omega}{\bar{v}}e_r(x,x')=0 \quad (37)$$

Where, $\gamma(x')=\alpha_n(x')v_n(x')n(x')+\alpha_p(x')v_p(x')p(x')$. Boundary conditions at n^+n and p^+p junctions are given by,

$$\left[-\frac{i\omega}{v_n}+D\right]e(x,x')=0 \qquad at \quad x=0 \quad (38)$$

$$\left[\frac{i\omega}{v_p}+D\right]e(x,x')=0 \qquad at \quad x=W \tag{39}$$

The noise electric field distribution along the depletion layer can be obtained by solving (36) and (37) subject to boundary conditions, (38) and (39), following the process described in [17].

In this analysis tunneling is assumed as a quiet or noiseless process. The avalanche process can be considered as combination of a noiseless generation rate G_A and a noise generation rate γ. An element of current dJ_n generated in the interval dx' around x' due to a noise generation source $\gamma(x')$ located at x' in the depletion layer.

$$dJ_n = q\gamma(x')dx' \tag{40}$$

From the theory of shot noise the element of mean-square noise current $\langle di_n^2 \rangle$ in a frequency interval df contributed by dJ_n is obtained,

$$\langle di_n^2 \rangle = 2q.df.dJ_n.A = 2q^2.df.\gamma(x').A.dx' \tag{41}$$

Where, A is the junction area of the device. By integrating $e(x,x')$ with respect to x within the whole depletion layer the terminal voltage $V_T(x')$ produced by $\gamma(x')$ can be obtained as,

$$V_T(x') = \int_0^W e(x,x')dx \tag{42}$$

Thus the transfer impedance can be defined as,

$$Z_T(x') = \frac{V_T(x')}{I_{N_{average}}(x')} \tag{43}$$

Where, $I_{Naverage}(x') = A\,dJ_n$ = the average current generated in the interval dx'. The mean-square noise voltage can be found as,

$$\langle v_n^2 \rangle = 2q^2.df.A\int |Z_T(x')|^2 \gamma(x')dx' \tag{44}$$

Mean-square noise voltage per bandwidth is called as Noise Spectral Density ($\langle v_n^2 \rangle/df$ $Volt^2.Sec$). The quantity, which can appropriately asses the performance of the diode in an amplifier is called noise measure. Noise measure can be defined [14, 28],

$$M = \frac{\langle v_n^2 \rangle / df}{4K_BT(-Z_R - R_p)} \tag{45}$$

Where, K_B = Boltzmann Constant, T = Absolute Temperature, Z_R = Diode negative resistance, R_p = Positive parasitic series resistance associated with the diode.

IV. Results and Discussions

A double iterative field maximum computer method is used by the authors where the basic device equations (e.g. Poisons Equation, Space Charge Equation and Current Continuity Equations) are solved simultaneously by considering the mobile space charge effect. An asymmetrically doped DDR MITATT diode is designed and optimized to operate near W-band. Structural and doping parameters of the diodes are tabulated in Table I and simulated DC and small-signal parameters are listed in Table II. Diode is assumed to operating in continuous wave (CW) mode. The impact ionization rates and carrier drift velocities and other material parameters for a semiconductor (silicon) are taken from recent reports [27] and incorporated in the analysis.

Doping profile of the diode is shown in Fig. 3. Fig. 4(a) and Fig. 4(b) show the electric field profile and $P(x)$ profile of the diode for bias current density $J_0 = 5\times10^8$ Amp/m^2. Small-signal conductance-susceptance plot and spatial variation of the negative resistivity (resistivity profile) (both for $J_0 = 5\times10^8$ Amp/m^2) are shown in Fig. 5 and Fig. 6 respectively.

TABLE I DIODE STRUCTURAL AND DOPING PARAMETERS

PARAMETER	VALUE
Diode Structure	Flat-DDR
Base Material	Silicon
n-epitaxial layer thickness (μm)	0.3200
p-epitaxial layer thickness (μm)	0.3000
n-epitaxial layer doping concentration ($\times10^{23}$ m^{-3})	1.450
p-epitaxial layer doping concentration ($\times10^{23}$ m^{-3})	1.750
n+-substrate layer doping concentration ($\times10^{26}$ m^{-3})	1.000

TABLE II SIMULATED DC AND SMALL-SIGNAL PARAMETERS

PARAMETER	VALUE
Bias Current Density, J_0 ($\times10^8$ Amp/m^2)	5.0
Peak Electric Field, E_m ($\times10^7$ $Volt/m$)	6.2998
Breakdown Voltage, V_B ($Volt$)	20.88
Efficiency, η (%)	9.34
Peak Operating Frequency, f_p (GHz)	122
Peak Conductance, G_P ($\times10^7$ S/m^2)	-6.4045
Peak Susceptance, B_P ($\times10^7$ S/m^2)	14.7890
Quality Factor, $Q = (-B_P/G_P)$	2.31
Negative Resistance, Z_R ($\times10^{-8}$ $Ohm.m^2$)	-0.2466
RF Power Output, P_{RF} ($Watt$)	0.3490

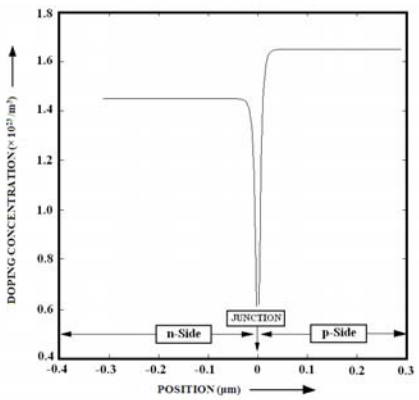

Fig. 3 Doping Profile of the Si based DDR MITATT diode.

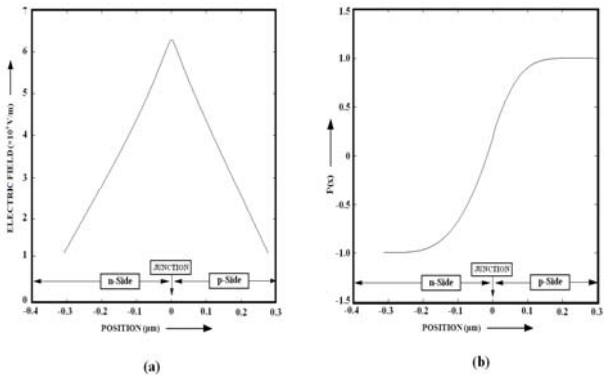

Fig. 4 (a) Electric field profile and (b) *P(x)* profile of the Si based DDR MITATT diode ($J_0 = 5\times10^8$ *Amp/m*^{2}).

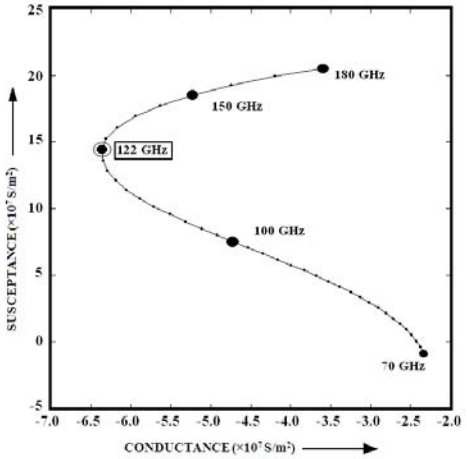

Fig. 5 Small-Signal Conductance-Susceptance plot of the Si based MITATT diode ($J_0 = 5\times10^8$ *Amp/m*^{2}).

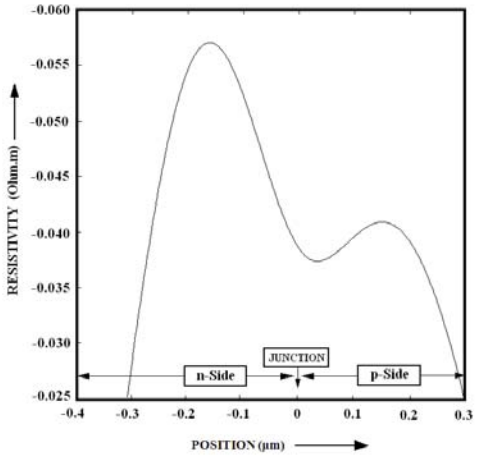

Fig. 6 Negative resistivity profile of the Si based MITATT diode ($J_0 = 5\times10^8$ *Amp/m*^{2}).

Now the effect of the tunneling current on the noise properties of MITATT device will be investigated (Figure 7). The results show some distinguishing features from those obtained for IMPATT device. According to Gummel and Blue [14], in IMPATT mode, with the increase of DC current density the mean-square noise voltage decreases in the low frequency region as well as near the resonant frequency. But in the case of MITATT mode of operation, it is seen that at the lower frequencies the variation of mean square noise voltage with DC current density is similar to the IMPATT mode. But unlike IMPATT mode, the peak of the spike increases as the operating current increases. It may be noted that as the operating current decreases (from 20×10^8 *Amp/m*^{2} to 5×10^8 *Amp/m*^{2}) the percentage of tunneling generation rate to the avalanche generation rate increases (from *1.28%* to *22.45%*) as shown in Table III which causes the peak of the spike to decrease. This trend shows that in MITATT mode the noise voltage would be totally dependent on the ratio of the peak tunneling generation rate to the peak avalanche generation rate (g_{Tpeak}/g_{Apeak}) instead of total DC current unlike the case in pure IMPATT devices [17].

TABLE III SIMULATED DC AND SMALL-SIGNAL PARAMETERS

Bias Current Density J_0 ($\times10^8$ *Amp/m*^{2})	Percentage of Tunneling Genration Rate g_{Tmax}/g_{Amax} *(%)*
20	1.28
15	2.89
10	7.18
5	22.45

The Noise Measure versus frequency is plotted for DC current density, $J = 5\times10^8$ *Amp/m*^{2} and various assumed values of parasitic positive series resistance for W-band Si DDR MITATT diode in Figure 8. It is clear that as the series resistance value increases Noise Measure also increases degrading the noise performance of the device. Figure 9 shows Noise Measure versus frequency curves for different current densities with $R_p = 0$ *Ohm*. As the current density increases the resonance frequency at which the Noise Measure is minimum increases, but the Noise Measure value at the corresponding resonance frequency decreases. These behaviors of the Noise Measure actually agree with results obtained by Gummel and Blue [14].

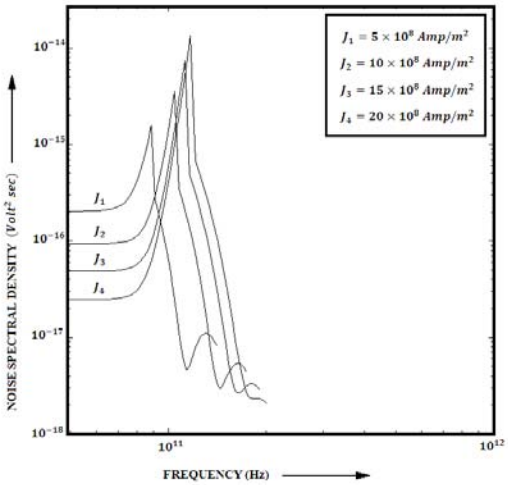

Fig. 7 The effect of operating bias current density on Noise Spectral Density ($\langle v_n^2\rangle/df$ *Volt*^{2}*.Sec*) versus frequency curves for the Si based MITATT diode.

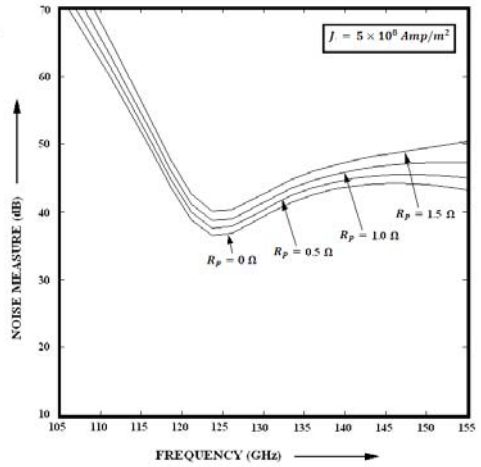

Fig. 8 Noise Measure versus frequency curves for DC current density, $J = 5 \times 10^8$ *Amp/m*^{2} and various assumed values of parasitic positive series resistance for the Si based MITATT diode.

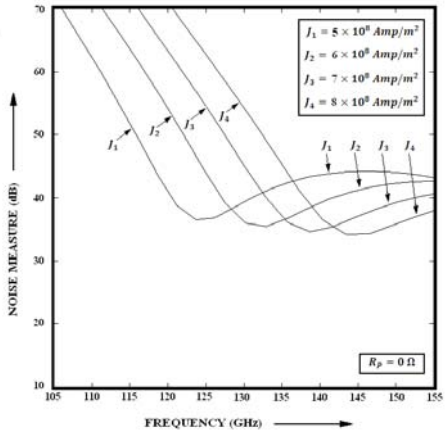

Fig. 9 Noise Measure versus frequency curves for different DC current densities (parasitic positive series resistance, $R_p = 0$ *ohm*) for the Si based MITATT diode.

From Fig. 9 it is clear that, noise measure decreases (improving the noise performance of the device) if bias current density increases. But at the same time by increasing bias current density the operating frequency of the device increases. So, there must be a trade-off between required noise performance and required frequency of operation while choosing the bias current density.

V. Conclusion

A generalized computer simulation method to analyze the noise generation process in MITATT device is presented in this paper. This method is applied to investigate the noise performances of a millimetre-wave Si based DDR MITATT device. The noise measure of the device at the operating frequency (122 GHz) with input power density of 10^{10} *Watt/m*^{2} is about *35 dB* for hypothetical series resistance value of zero ohm (estimated junction temperature = *500 K*). Results show that as the series resistance associated with the device increases, noise performance of the device deteriorates by increasing the noise measure value at the operating frequency. The investigations also show that the increase in the tunneling generation rate decreases the noise levels of MITATT diodes.

References

[1] T. A. Midford and R. L. Bernick, "Millimeter Wave CW IMPATT diodes and Oscillators", IEEE Trans. Microwave Theory Tech., vol. 27, pp. 483-492, 1979.

[2] Y. Chang, J. M. Hellum, J. A. Paul and K. P. Weller, "Millimeter-Wave IMPATT Sources for Communication Applications", IEEE MTT-S International Microwave Symposium Digest, pp. 216-219, 1977.

[3] W. W. Gray, L. Kikushima, N. P. Morentc and R. J. Wagner, "Applying IMPATT Power Sources to Modern Microwave Systems". IEEE Journal of Solid-State Circuits, vol. 4, pp. 409-413, 1969.

[4] M. Mukherjee and N. Mazumder, "Effect of charge-bump on high-frequency characteristics of α-SiC based double drift ATT diodes at MM-wave window frequencies", IETE J. of Research, vol. 55, pp. 118-127, 2009.

[5] G. N. Dash and S. P. Pati, "A generalized simulation method for MITATT-mode operation and studies on the influence of tunnel current on IMPATT properties", Semicond. Sci. Technology, vol. 7, pp. 222-230, 1992.

[6] M. Mukherjee and N. Mazumder, "Comparison of photo sensitivity of Si and InP IMPATT diodes at 220 GHz", Proc. of IEEE International conference on Microelectronics, Electronics and Electronic Technologies (IEEE-MEET 2007), University of Zagreb, Croatia, pp. 72-77, 2007.

[7] J. P. Banerjee, S. P. Pati and S. K. Roy, "Computer simulation experiment on the mm-wave properties of InP double drift IMPATTs", Phys. Status Solidi, vol. 109, pp. 359-364, 1988.

[8] M. Mukherjee, S. Banerjee and J. P. Banerjee, "Dynamic characteristics of iii-v and iv-iv semiconductor based transit time devices in the terahertz regime: a comparative analysis", Terahertz Science and Technology, vol. 3, pp. 97-109, 2010.

[9] M. J. Bailey, "Heterojunction IMPATT diodes", IEEE Transactions on Electron Devices, vol. 39, issue 8, pp. 1829-1834, 1992.

[10] J. C. de Jaeger, R. Kozlowski, G. Salmer, "Expected performances of GaAlAs/GaAs double-velocity heterojunction impatt diodes", Electronics Letters, vol. 20, issue 19, pp. 803-804, 1984.

[11] J. K. Mishra, A. K. Panda, G. N. Dash, "An extremely low noise heterojunction IMPATT", IEEE Transactions on Electron Devices, vol. 44, issue 12, pp. 2143-2148 , 1997.

[12] A. S. Tager, "Current fluctuations in semiconductor (dielectric) under the conditions of impact ionosation and avalanche breakdown" Sov. Phys. Solid State, vol. 4, pp. 1919, 1965.

[13] M. E. Hines, "Noise theory of Read type avalanche diode", IEEE Trans. Electron Devices, vol. ED-13, pp. 57, 1966.

[14] H. K. Gummel and J. L. Blue, "A Small-Signal Theory of Avalanche Noise in IMPATT Diodes", IEEE Trans. Electron Devices, vol. ED-14, No. 9, pp. 569-580, 1967.

[15] H. A. Haus, H. Statz and R. A. Pucel, "Optimum noise measure of IMPATT diode", IEEE Trans. on MTT, vol. MTT-19, pp. 801, 1971.

[16] R. L. Kuvas, "Noise in IMPATT diodes Intrinsic properties", IEEE Trans. Electron Devices, vol. ED-19, pp. 220, 1972.

[17] G. N. Dash, J. K. Mishra and A. K. Panda, "Noise in Mixed Tunneling Avalanche Transit Time (MITATT) diodes", Solid-State Electronics, vol. 39, no. 10, pp. 1473-1479, 1996.

[18] S. K. Roy, J. P. Banerjee and S. P. Pati, "Computer methods for the dc field and carrier current profiles in impatt devices starting from the field extremum in the depletion layer", Proc. of NASECODE-I Conf. on Numerical Analysis of Semiconductor Devices (Dublin: Boole Press), pp. 266, 1979.

[19] S. K. Roy, J. P. Banerjee and S. P. Pati, "A computer analysis of the distribution of high frequency negative resistance in the depletion layers of impatt diodes", Proc. of NASECODE-IV Conf. on Numerical Analysis of Semiconductor Devices (Dublin: Boole Press), pp. 494, 1985.

[20] M. Mukherjee and J. P. Banerjee, "DDR Pulsed IMPATT Sources at MM-Wave Window Frequency: High-Power Operation Mode", International Journal of Advanced Science and Technology, vol. 19, pp. 1-11, 2010.

[21] M. Sridharan and S. K. Roy, "Computer studies on the widening of the avalanche zone and decrease on efficiency in silicon X-band sym. DDR", Electron Lett., vol. 14, pp. 635-637, 1978.
[22] M. Sridharan and S. K. Roy, "Effect of mobile space charge on the small signal admittance of silicon DDR", Solid State Electron, vol. 23, pp. 1001-1003, 1980.
[23] M. E. Elta, "The effect of mixed tunneling and avalanche breakdown on microwave transit-time diodes", Ph.D. dissertation, Electron Physics Lab., Univ. of Mich., Ann Arbor, MI, Tech. Rep, 1978.
[24] E. O. Kane, "Theory of tunneling", J. Appl. Phys., vol. 32, pp. 83-91, 1961.
[25] Canali, C., Ottaviani, G., and Quaranta, A. A., "Drift velocity of electrons and holes and associated anisotropic effects in silicon", J. Phys. Chem. Solids, vol. 32, pp. 1707-1720, 1971.
[26] D. L. Scharfetter and H. K. Gummel, "Large-Signal Analysis of a Silicon Read Diode Oscillator", IEEE Trans. on Electron Devices, vol. 16, pp. 64-77, 1969.
[27] 'Electronic Archive: New Semiconductor Materials, Characteristics and Properties', http://www.ioffe.ru/SVA/NSM/Semicond.
[28] H. A. Haus and R. B. Adler, "Circuit Theory of Linear Noisy Networks", New York: Willy, 1959.
[29] J. F. Luy, A. Casel, W. Behr and E. Kasper, "A 90-GHz double-drift IMPATT diode made with Si MBE", IEEE Trans. Electron Devices, vol. 34, pp. 1084-1089, 1987.